

FINITE ELEMENT MODELING OF PULSED EDDY CURRENT PHENOMENA

Bruce L. Allen and W. Lord

Colorado State University
Electrical Engineering Department
Fort Collins, Colorado 80523

INTRODUCTION

Conventional eddy current methods, using single-frequency excitation employ instruments which monitor the phasor value of the impedance, or impedance plane trajectory. Changes in the test specimen or test conditions result in a change in the value of the impedance. The monitored value of the impedance traces out loci which are generally unique to the cause of the change in impedance. In the event that a change in test conditions produces a locus similar to a locus produced by a change in the test specimen, an alternative test must be developed.

Multifrequency eddy current methods provide an alternative approach. The effects of changes in test conditions such as probe liftoff can be negated by a multiplication and rotation of the liftoff locus in one frequency, and subtraction of the resultant impedance from the locus in another frequency.

Pulsed eddy current techniques offer another testing alternative by monitoring a different type of test signal. Rather than observing changes in impedance of an eddy current coil, the pulsed eddy current test measures the emf induced across test coils.

A variety of test systems have been used in pulsed reflection eddy current testing [1,2].

Through-transmission systems have also been implemented by Renken [4]. The through-transmission setup consists of a single field coil which transmits a pulsed field through a conductive specimen and induces a voltage in a pickup coil located on the opposite side of the medium as shown in Figure 1. Both through-transmission and reflection systems rely on the use of masks to improve resolution while maintaining magnetic field densities. The mask apparatus is a copper shield which confines the EM field to a desired size by an

aperture in the shield which confines the path which the field must take to interact with the test specimen.

Overall, pulsed eddy currents have seen sparse application as a nondestructive testing tool. The lack of an analytical model for the design of probes, probe masks and the tests themselves has possibly hindered the advancement and utilization of the technique.

In recent literature, finite element methods have been used to model single frequency eddy current nondestructive tests of nuclear steam generator tubes [5]. Finite element methods have also been used to model active and residual leakage fields [6].

The extension of finite element techniques into the area of pulsed eddy current problems appeared to be feasible and useful and is the motivation behind this work.

Two approaches are used to model the simple through-transmission setup of Figure 1. If the field coil is excited by a current pulse train, a series of steady state solutions can be performed for each of the significant sinusoidal harmonics contained within the pulse waveform. Superposition of results is then used to determine the overall solution.

A second approach is used to solve the problem when the field coil is excited by a single current pulse. The solution approach to this problem is to utilize an iterative time stepping algorithm. Thus, the first problem is solved in terms of steady state phasors, while the second problem is solved in a transient state.

Experimental results are provided to validate and test the finite element codes.

EXPERIMENTAL RESULTS

The test setup of Figure 1 is attractive from the standpoint of its simple axisymmetric geometry. Through-transmission tests were performed on both 1/4 inch stainless steel plate and 1/16 inch aluminum plate. The emf signals observed across the pickup coil are indicative of the conductive medium which diffuses the pulsed EM

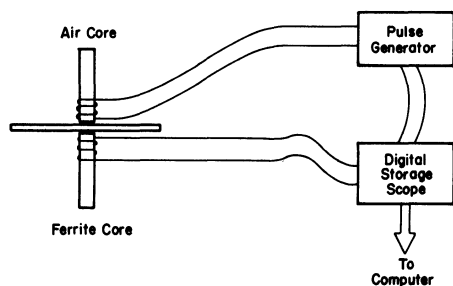


Figure 1
Through-transmission System

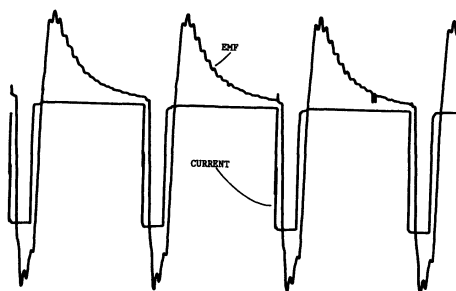


Figure 2
Real Time Signals

field. The amplitude of the emf waveform and the time delay in the arrival of the signal energy contain information about the test specimen and the test conditions.

The amplitude level is sensitive to probe liftoff, but the time delay remains unaffected since the signal velocity in air is in excess of 5 orders of magnitude greater than the signal velocity within the metal specimen.

To assess accurately the time delay between the emf signal and the current pulse under multiple pulse excitation, both the emf and current waveforms were sampled and stored on a Nicolet digital oscilloscope. Transfer of the data to a VAX 11/780 computer was accomplished via an 8080 based Vector microcomputer. The data files created on the VAX by the transfer were processed using a cross correlation algorithm. In addition a power spectrum estimate was made of the current pulse waveform to determine which harmonics within the signal comprise the bulk of the signal energy. This information is used later in determining which harmonics should be included in the finite element solution.

Figure 2 is a sample of the current waveform and the emf waveform for 1/4 inch stainless steel plate. For the signals shown, a current pulse width of 20 μ sec duration operating at a pulse repetition frequency (PRF) of 10 kHz was used. The peak value of the current is 0.5 amperes flowing in a low inductance air core field coil with a 1/4 inch core diameter. A ferrite core pickup coil, also 1/4 inch in diameter is used to improve the turn's flux linkages and aid in developing substantial emf levels.

The power spectrum of the sampled current waveform was determined, and the first nine harmonics contained the vast majority of the signal energy. Thus the first nine harmonics are the frequencies at which a steady state solution is conducted.

The cross correlation of the two signals is performed in the frequency domain using a FFT algorithm. The resulting cross correlogram exhibited a shift of 6 μ sec in the positive peak value of the correlogram. This shift is the time delay in the correlation of the two signals and is used as the main method of comparison between finite element and experimental results for the steady state solution.

To evaluate the results of the transient time stepping program, single shot current pulse tests were conducted. Time signals were sampled for a single current pulse of 5 μ sec duration with the test specimen again being stainless steel.

FINITE ELEMENT MODELING

The governing equation of the problem is that of the diffusion equation [7],

$$\frac{1}{\mu} \nabla^2 \bar{A} = -\bar{J}_s + \sigma \frac{\partial \bar{A}}{\partial t} \quad (1)$$

where \bar{J}_s is the source current density, σ the material conductivity, μ the permeability, and \bar{A} the magnetic vector potential. A solution of the magnetic vector potential throughout the region is the first step to predicting the voltage signal in the pickup coil.

The geometry is discretized by a mesh of triangular elements and a solution of the magnetic vector potential is obtained at each node. Rather than solve equation (1), an energy functional which equivalently describes the problem is minimized using variational calculus.

$$\bar{J} = \int_s \left\{ \frac{1}{2\mu} \left\{ \left| \frac{\partial \bar{A}}{\partial r} + \frac{\bar{A}}{r} \right|^2 + \left| \frac{\partial \bar{A}}{\partial z} \right|^2 \right\} + \sigma \frac{\partial \bar{A}}{\partial t} \cdot \bar{A} - \bar{J}_s \cdot \bar{A} \right\} \partial V \quad (2)$$

For the case that \bar{A} is a steady state sinusoidal field with angular frequency ω , Euler's identity may be used to express \bar{A} . Thus the second term in equation (2) becomes,

$$\frac{j\sigma\omega}{2} |\bar{A}|^2$$

For the case that \bar{A} is a transient field, the term $\partial \bar{A} / \partial t$ must be treated as a separate function in the solution of \bar{A} .

STEADY STATE FORMULATION

In solving for \bar{A} when the field coil is excited by a current pulse train, the function \bar{A} can be expressed by Euler's identity.

$$\bar{A} = A_0 e^{-j\omega t}.$$

A_0 is a function of r and z , ω corresponds to the frequency of the harmonic for which a solution is performed, and \bar{A} has only a θ component as does the source current density. The minimization of the energy, J leads to the complex finite element equation [8].

$$[SK]\{\bar{A}\} = \{\bar{Q}\} \quad (3)$$

The contents of the complex $[SK]$ matrix (global stiffness matrix) arise from a piecewise integration, element by element, of the mesh. The $\{\bar{Q}\}$ or source matrix contains the source current density distributed at each of the nodes which comprise the elements modeling the field coil windings.

The Gaussian elimination technique is used to solve the set of simultaneous equations which comprise equation (3). Once the solution for \bar{A} is performed, the utilization of the linear approximating functions used in the solution of the magnetic vector potential at each nodal point allows the value of \bar{A} to be determined at any point within an element. The approximating function is simply evaluated at the coordinates of the point and multiplied by the nodal point values of the magnetic vector potential.

$$\bar{A}(r, z) = [N_i(r, z)]\{A_i\} \quad (4)$$

From the nodal point values of \bar{A} , the value of \bar{B} can be found from the approximating functions, N by applying equation (5).

$$\bar{B} = \nabla \times \bar{A} \quad (5)$$

Thus, the application of the curl to the approximating functions allows the magnetic flux density to be evaluated.

$$\bar{B}(r, z) = [\nabla \times N_i(r, z)]\{A_i\} \quad (6)$$

Once \bar{B} is known at each element in the region of the pickup coil windings, the total flux linkages can be found. Then the emf induced in the pickup coil can be found by reincorporating time into the phasor value of the magnetic flux. The entire solution procedure is repeated for each harmonic and superposition of results is used to estimate the emf waveform.

Figure 3 shows a contour plot of the flux lines ($|\bar{A}|$) for the fundamental harmonic in stainless steel. Figure 4 is the predicted emf waveform and a simulated pulse waveform based on the Fourier series coefficients of the current pulse waveform.

A cross correlation of the two signals in Figure 4 was performed using the same algorithm that was used for the experimental signals. The shift in the peak, or time delay was 6.0 μsec which is the same as the experimental results. Solutions were also performed for aluminum as the test medium, but a discrepancy of 3 μsec existed between experimental and finite element results. This difference in results is believed to be the effects of element density within the mesh. It is noted that in the conducting medium of the mesh, the best results occur if 2 divisions of elements are used for each depth in the material equal to the material's skin depth. Since a variety of skin depths occur (depending upon which harmonic solution is being performed) a series of mesh densities would be required.

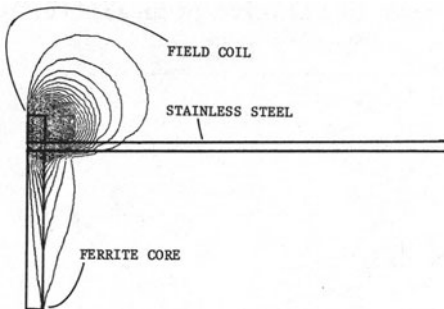


Figure 3
Flux Plot

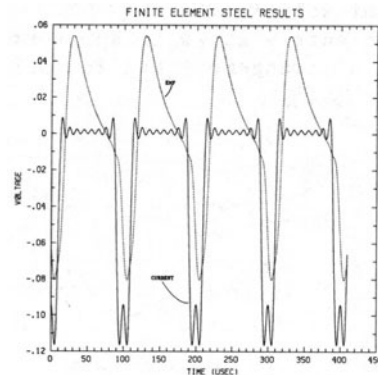


Figure 4
F.E. Prediction of EMF in Pickup Coil

TRANSIENT FORMULATION

The minimization of the energy functional of equation (2) leads to [9]

$$[S]\{\bar{A}\} = \{\bar{Q}\} - [C]\{\dot{\bar{A}}\}. \quad (7)$$

To solve the matrix equation for \bar{A} , an approximation of $\dot{\bar{A}}$ must be made at each time step. A backward difference approximation is used which maintains a stable solution. The approximation is:

$$\dot{\bar{A}}(t+\Delta t) = \frac{\bar{A}(t+\Delta t) - \bar{A}(t)}{\Delta t}. \quad (8)$$

The approximation contains $\bar{A}(t+\Delta t)$ which is the quantity equation (7) solves for. This portion of the approximation enters the left hand side of equation (7) as shown in equation (9). Thus the approximation enters the finite element equation explicitly.

Assembly of the matrices of equation (7) is accomplished by performing a piecewise integration. In the transient program an isoparametric element is used, and the integration procedure over each element is accomplished using Gaussian quadrature.

The solution of the simultaneous equations is again achieved through Gaussian elimination. The LDU matrix decomposition which occurs during the Gaussian elimination process, greatly adds to the efficiency of the iterative solution. This is because only the right hand side of equation (7) changes from one iteration to the next. Thus, once an LDU decomposition is performed for the first iteration, only a forward substitution and backward substitution are required to obtain a solution for each succeeding iteration.

Figure 5 is a comparison of the experimental emf waveform to the transient finite element prediction. The two waveforms are normalized to the same peak negative value to overcome magnitude discrepancies. Good waveshape and time delay are predicted by the finite element solution.

Figure 6 shows an apparent sensitivity that the through-transmission arrangement has to small changes in relative permeability

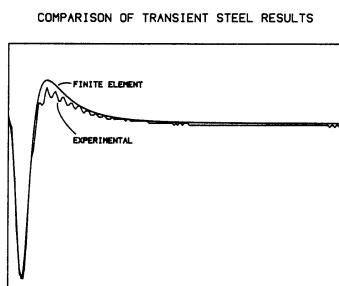


Figure 5
Comparison of Results

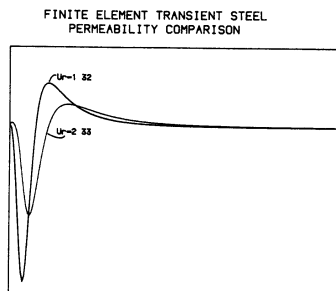


Figure 6
Sensitivity to Permeability

in the test specimen. A change in the relative permeability in the stainless steel sample from the measured value of 1.32 to a random value of 2.33 drastically reduces the signal amplitude and slows the diffusion process.

The sequence of plots in Figure 7 corresponds to the flux lines at sequential time steps as the signal diffuses through the conductive medium. The field lines above the steel plate have been suppressed, focusing on the flux lines in the region of the steel plate and the pickup coil. These geometries are outlined in the contour plots.

The first contour plot, at 5 μsec , is at the time when the current pulse in the field coil is just shutting off. The contours are obviously closed about the field coil. In the next two sequences, the flux lines are drawn down into the ferrite core of the

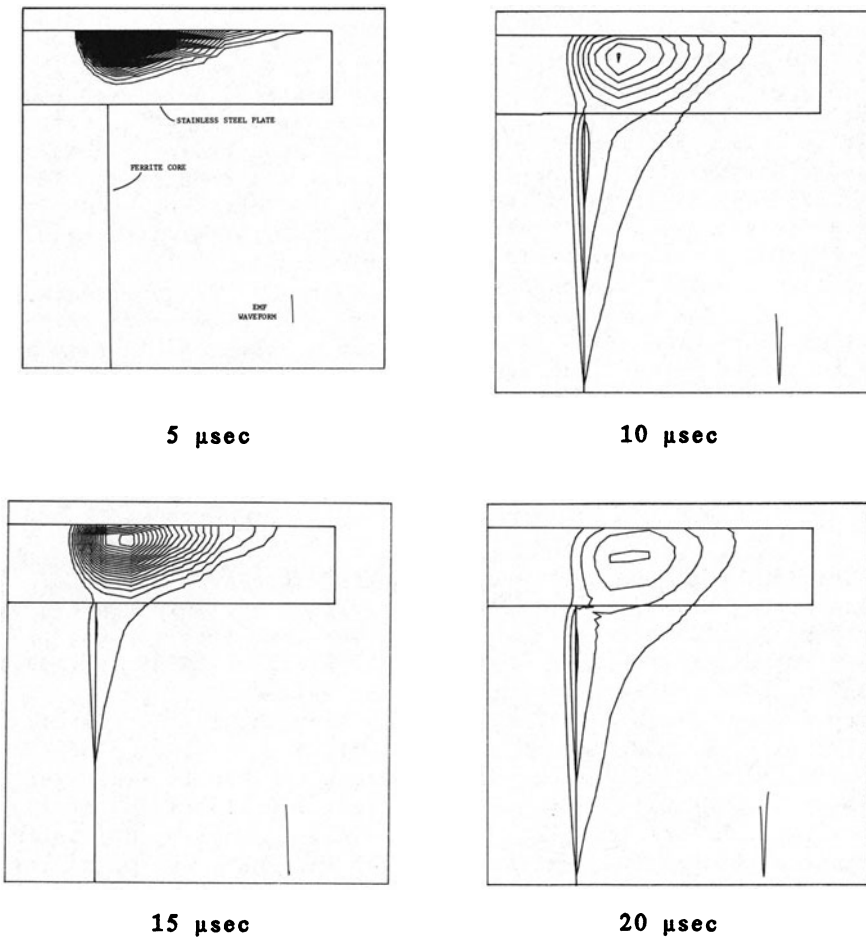


Figure 7
Transient Flux Plots

pickup coil. The progression of the emf waveform is also shown in the bottom right hand corner of each plot. The emf peaks when the rate at which the flux linkages are increasing reaches a maximum. The emf crosses zero when the flux linkages starts to decrease. The positive peak in the emf is rather broad, and indicates the peak rate at which the flux linkages are decreasing.

CONCLUSION

The application of finite element techniques to the field of pulsed eddy currents has been investigated. Two approaches have been taken in arriving at solutions of the magnetic vector potential.

A steady state solution is performed for each of the harmonics described by the Fourier series of a current pulse train. Superposition of the set of steady state solutions is used to determine the overall solution.

A second approach solves the problem as a transient system using a time stepping iterative solution for a single current pulse.

Both programs predict the emf waveform which is induced across the pickup coil. The results of the steady state solution were affected by a variation in mesh density for each harmonic, but an accurate time delay of the diffusion process was predicted. The transient program accurately predicted the emf waveshape and time delay, however both programs failed to predict the magnitudes in the emf signal which were observed experimentally.

Overall, a first approach to the modeling of the pulsed eddy current phenomena shows the finite element method to be applicable to the problem. However, an understanding of the variation in magnitudes must be reached, and an extension of the technique to pulsed reflection systems would allow practical applications to be simulated.

REFERENCES

1. Waidelich, D.L., Measurement of coating thickness by use of pulsed eddy currents, *Materials Evaluation* 14:14-16 (1956).
2. Sather, A., Pulsed eddy current testing apparatus for use on smooth and ribbed tubing, *Materials Evaluation* 35:55-59 (1977).
3. Renken, C. J., A through transmission system using pulsed eddy current fields, *Materials Evaluation* 18:234-236 (1960).
4. Palanisamy, R. and Lord, W., Finite element simulation of support plate and tube defect eddy current signals in steam generator NDT, *Materials Evaluation* 39:651-655 (1981).
5. Satish, S. R. and Lord, W., Finite element modeling of residual magnetic phenomenon, Presented at the international magnetics conference, Boston, April 1980.
6. Brauer, J. R., Finite element analysis of electromagnetic induction in transformers, Presented at the IEEE Winter Power Meeting, N.Y., January 1977.